The Tropical Cyclone Diurnal Cycle

A prospectus presented to the doctoral committee in
partial fulfillment of the requirements for the degree
of Doctor of Philosophy

College of Arts and Sciences Department of Earth
and Atmospheric Science University at Albany
State University of New York

Jason P. Dunion
Spring 2013

1.Introduction

Although numerous studies have documented the existence of diurnal maxima and minima associated with tropical oceanic convection and the tropical cyclone (TC) upper-level cirrus canopy, we lack a thorough understanding of the nature and causes of these variations and especially the extent to which these variations are important for TCs. It is well known that the coherent diurnal cycle of deep cumulus convection and associated rainfall is different over the land and ocean (Gray and Jacobson, 1977, Yang and Slingo, 2001). While over the land it tends to peak in the late afternoon-early evening due to daytime boundary layer heating, over the ocean it peaks in the early morning (Fig. 1). In addition, Gray and Jacobsen (1977), Mapes and Houze (1993), and Liu and Moncrieff (1998) found that the oceanic peak was more prominent when the pre-existing convection was more intense and associated with an organized weather system such as an African easterly wave or mesoscale convective system. Numerous studies have also highlighted diurnal changes in the cirrus anvils of tropical deep convection and TCs. Weikmann et al (1977) noted that anvils emanating from large cumulonimbus clouds tended to grow preferably between 2200-0300 LST. Browner et al (1977) found that the areal extent of the TC cirrus canopy was a minimum at 0300 LST and a maximum at 1700 LST and suggested that this diurnal oscillation might be important for the TC (Fig. 2). More recently, Kossin (2002) used storm centered GOES infrared (IR) imagery to calculate azimuthally averaged brightness temperatures and create Hovmoller-type diagrams of brightness temperature diurnal oscillations over time. That study concluded that although a clear diurnal oscillation of the TC cirrus canopy was present at larger radii (e.g. 300 km), few storms exhibited diurnal oscillation signals in their innermost 100 km. It was hypothesized that different processes might be forcing periodic oscillations in the TC deep inner core convection and the TC cirrus canopy. This dissertation

aims to shed more light on these TC diurnal oscillations and to suggest possible mechanisms to explain them. Various aspects of the TC diurnal cycle will be explored using a combination of satellite data, aircraft observations, and model analyses.

This study takes a novel satellite-based approach to observing diurnal oscillations in TCs and finds an intriguing diurnal pulsing pattern that appears to occur with remarkable periodicity through a relatively deep layer of the TC. Storm-centered GOES IR imagery (10.7 μm) was used to create 6-h brightness temperature difference fields of the storm environment. The imagery reveals a cool ring (i.e. local cooling of the brightness temperatures over time) that begins forming in the storm's inner core near the time of sunset each day. This cool ring feature (hereafter referred to as a diurnal pulse) continues to move away from the storm overnight, reaching areas several hundred kilometers from the circulation center by the following afternoon. A marked warming of the cloud tops occurs behind this propagating feature and there appears to be significant structural changes to a storm as it moves away from the inner core. This suggests that diurnal pulses may are a distinguishing characteristic of the TC diurnal cycle and may have important implications for TC intensity change. A comprehensive dataset of all North Atlantic major hurricanes from 2001-2010 is developed and used to examine the mean characteristics of the TC diurnal cycle in the TC environment. Preliminary research also suggests the presence of a diurnal signal in UW-CIMSS objective Dvorak intensity estimates and upper-level (150-300 hPa) divergence analyses for the 10-yr North Atlantic major hurricane dataset. The nature of these embedded diurnal signals will be examined in detail using the 10-yr TC dataset and possible implications explored.

NOAA G-IV hurricane hunter missions conducted NOAA/HRD's Tropical Cyclone Diurnal Cycle (TCDC) Experiment around Hurricane Katia on 06 and 07 September 2011 and

collected detailed observations (GPS dropwindsondes and tail Doppler radar data) of diurnal pulses moving out from the storm during this 48-hr period. Data from these two missions will be examined in detail to investigate the atmospheric signals associated with TC diurnal pulses and improve our understanding of these features. It is anticipated that additional tropical cyclone diurnal cycle observations that will be collected by NOAA (P-3 Orions and G-IV jet) and NASA (Global Hawks) during the 2013 Atlantic hurricane season will also be incorporated into this dissertation. Specific effort will be made to sample TC diurnal pulses during various stages of their evolution [i.e. at both smaller radii (<200 km, just after sunset) and larger radii (300-500 km) several hours after sunset] and throughout the depth of the TC environment, including the upper-level cirrus canopy.

Preliminary analyses from a Hurricane Nature Run (Nolan et al. 2013) indicate that the TC diurnal cycle is detectable in the high-resolution model output analyses of radiation tendency, q condensate and vertical motion. An in-depth examination of the simulated kinematic, thermodynamic, and radiative components of the Hurricane Nature Run and the TC diurnal cycle will be examined and incorporated into this work. Output from a WRF TC simulation will be also used to examine various aspects of the TC diurnal cycle. Finally, the Three Dimensional Vortex Perturbation Analysis and Simulation (3DVPAS) model will be utilized to conduct sensitivity experiments (e.g. radiation and thermodynamics) to examine various aspects of TC diurnal cycle formation and evolution.

While the exact processes that cause the TC diurnal cycle and associated diurnal pulses remain uncertain, a combination of satellite data, aircraft observations, and model simulations will be used to examine several hypotheses that could explain their development and evolution. The remarkable predictability (timing and propagation) of the TC diurnal cycle provides an

important means for advancing our understanding of this phenomenon in the future. This predictability suggests that satellite imagery could readily be used to anticipate diurnal pulse evolution in the TC environment, provide guidance for monitoring possible impacts on the storm, and guide aircraft sampling of its structure. Additionally, the apparent diurnal cycle signal in the TC nature run will provide a robust means for testing the hypotheses that are posed in this project. The repeatability of TC diurnal pulsing in time and space in various global basins suggests that it may be an unrealized, yet fundamental TC process.

This dissertation will aim to address the following science questions:

i. What are the spatial and temporal characteristics of the TC diurnal cycle?
ii. What remote sensing techniques can be developed/utilized to track the TC diurnal cycle in time and space?
iii. What are the physical mechanisms responsible for the onset and evolution of the TC diurnal cycle?
iv. What is the influence of the diurnal cycle on TC upper-level outflow and divergence?
v. To what extent are diurnal variations important for TC track, intensity, and structure?
vi. What are the implications of the TC diurnal cycle on the structure and intensity of TCs, African easterly waves, and tropical convection in general?

2. Data and Methods

This study will utilize a combination of satellite data, aircraft observations, and model simulations to investigate the nature of the TC diurnal cycle and are outlined in detail below.

a. Satellite data

i. GOES Infrared Satellite Imagery

Three-hourly GOES 4-km IR (10.7 μm) imagery will be examined for all Atlantic major hurricanes from 2001-2010 and includes over 850 satellite images for 36 TCs. Each storm-centric image was geo-located using a combination of National Hurricane Center Best track data, aircraft center positions, and (when an eye was present) positions determined manually using the

Man-computer interactive data access system (McIDAS). Two types of storm centered IR imagery are examined in detail: standard 10.7 μm imagery and 6-hr brightness temperature differencing imagery. The latter is created by differencing the brightness temperature fields of two consecutive 6-hr storm centered 10.7 μm IR images. The resulting satellite image has utility for quantifying brightness temperature changes in the TC environment and for monitoring structural changes in the TC cirrus canopy, eye, and regions of deep convection (in areas not obscured by the cirrus canopy). Azimuthal means of the IR brightness temperatures and 6-hr IR brightness temperature differences are calculated every 3-hr at 100 km radius intervals (100-600 km) for each storm in the 10-yr dataset. This information provides a means to monitor diurnal variations in the brightness temperature fields of the various storm environments. Other IR brightness temperature differencing increments (e.g. 3-hr) and satellite channels (e.g. the 6.8 μm water vapor channel) will also be examined.

It is hypothesized that various environmental and physical effects could impact the robustness of the observed TC diurnal cycle. For example, the IR satellite imagery that will be employed in this study typically detects high-level cirrus in the TC canopy and embedded deep convection. Therefore, in cases of moderate to high shear (e.g. >7.5 m s^{-1}), asymmetries in the observed satellite cloud field will often occur and may not necessarily reflect the typical TC outflow pattern. Additionally, terrain-induced convection (e.g. related to frictional convergence and surface heating) in the periphery of TCs near land can promote convective development that may not be representative of a TC's natural convective patterns. Finally, weak or insipient TCs often exhibit sporadic and/or asymmetric convective activity that may not reflect the natural convective cycles that are inherent in mature TCs. Based on these considerations, the following criteria will be used to subsample each 3-h cycle for the storms in the 10-yr dataset: 1) 200-850

hPa vertical wind shear ≤7.5 m s^{-1} [determined from the Statistical Hurricane Intensity Prediction Scheme (SHIPS)]; 2) storm center ≥300 km from land; and 3) Saffir-Simpson storm intensity of category 2 or higher (≥42 m s^{-1}). Finally, a continuous 72-h period is identified for each TC that is roughly centered around the storm's peak intensity while also maximizing the number of usable azimuthal calculations (given the three selection criteria discussed above). A 72-h time window is chosen based upon the fact that North Atlantic major hurricanes only maintain category 3 or higher intensity for an average of ~2.5 days (Jarvinen et al. 1984). The selection criteria described above results in 450 individual 3-hourly brightness temperature/brightness temperature difference azimuthal calculation sets for 31 North Atlantic major hurricanes from 2001-2010.

ii. Microwave Satellite Imagery (37 and 85/89/91 GHz)

Microwave satellite imagery from the 37 and 85/89/91 GHz channels on the NASA Aqua and DMSP satellites will be used to compliment the GOES IR imagery and examine the storm structure below the cirrus canopy for select TC cases in this study. For the 85 GHz wavelength, the TC cirrus canopy is largely transparent, while scattering by snow and ice above the freezing level is readily detectable. Therefore, this channel is ideal for examining TC inner core and rainband structures in the middle to upper levels. The 37 GHz channel can also detect emissions from below cirrus canopy, but is also much less sensitive to precipitation-sized ice particles and more sensitive to low-level rain. Therefore, this channel has utility for detecting lower to middle level features in the storm environment. Together, the 85 and 37 GHz channels elucidate important details regarding the nature of the TC diurnal cycle that is being detected in the GOES IR imagery and provide information as to the approximate depth of the observed diurnal pulses.

Since one of the main objectives of this effort is to identify diurnal variability in the TC environment, it is necessary to adjust the 10-yr dataset into a local standard time (LST) framework. It is hypothesized that radiative responses at the cirrus canopy level near the time of sunset may be a critical driving mechanism for the TC diurnal cycle. This would suggest that the time of local sunset governs the evolution of the TC diurnal cycle processes described here. Since this time can vary by ~3 hr across the North Atlantic basin from 01 June – 30 Nov, azimuthal calculations of IR brightness temperatures and 6-h IR brightness temperature differences performed relative to local sunset are probably the most robust way to represent the TC diurnal cycle. However, because LST provides a more familiar baseline, mean statistics relative to both LST and hours after sunset will be presented.

iii. UW-CIMSS Advanced Dvorak Technique

The Advanced Dvorak Technique (ADT) represents an automated version of the operational Dvorak Technique for estimating TC intensity (Olander and Velden 2007). The algorithm utilizes 11 μm IR imagery from geostationary satellites to examine various kinematic (e.g. vorticity and vertical wind shear) and thermodynamic (e.g. convective activity and core temperature) properties of the TC cloud pattern to produce a current intensity (CI) number ranging from 1.0-8.0. This value is empirically converted to an equivalent maximum sustained surface wind and a wind-pressure relationship is then used to assign the corresponding minimum sea level pressure (Velden et al. 2006). Two parameters that are produced in the operational ADT output include the raw tropical ("T") number and the current intensity (CI) number. The former intensity estimate is determined from the current Dvorak scene type (e.g. eye, central dense overcast, embedded center, curved band, and shear) and measured environmental parameters (e.g. scene temperatures and symmetry in the eye and cloudy regions of the storm)

and has a final value that is not constrained in any way. The latter value is derived from the initial raw T number, but also includes operational rules and constraints that define how much a T number can change over a specified time interval, given an observed storm structure in the satellite imagery. Analyses will be performed on the 2001-2010 major hurricanes examined in this dissertation to assess whether a coherent diurnal signal exists in the Dvorak satellite estimates (T numbers and CI numbers) that are routinely used to determine TC intensity in ocean basins around the world.

iv. UW-CIMSS Upper-Level Divergence Analyses

UW-CIMSS produces a real-time upper-level (150-300 hPa) divergence satellite product that includes analyses of the TC environment (Fig. 3). These products utilize NAVY NOGAPS model background fields and integrate satellite water vapor and IR winds into the analysis domain using a recursive filtering technique. The gridded analyses will be converted to McIDAS AREA files and azimuthal calculations of divergence will be made at various radii from the storm center (e.g. R=0-600 km). Preliminary examinations of 2005 Hurricane Emily and 2010 Hurricane Earl (not shown) suggest that upper-level divergence over the storms did indeed exhibit diurnal variability. The full 10-yr TC dataset will be investigated to determine whether a robust, coherent diurnal signal of upper-level divergence exists in the TC environment and how that signal varies in time and space.

b. Aircraft Observations

i. 2011 Aircraft Field Campaign

NOAA/HRD conducted two TC Diurnal Cycle Experiment missions into Hurricane Katia (06 and 07 September) with the G-IV high altitude jet. The main objectives of these two

missions included sampling TC diurnal pulses and atmospheric moisture in the environment of Katia using GPS dropwindsondes and the new G-IV tail Doppler radar. Approximately 30 GPS dropwindsondes were launched during each mission and each vertical profile includes pressure, temperature, moisture, and wind information from ~41,000-45,000 ft to the surface with a vertical resolution of ~5 m. The G-IV tail Doppler radar was fully operational during the 06 September mission, but was not functioning during the second mission. The G-IV tail Doppler radar data from 06 September mission will potentially provide important information regarding the 3-dimensional wind field and distribution of radar reflectivity in the environment of Hurricane Katia.

ii. 2013 NOAA and NASA Aircraft Field Campaigns (Anticipated)

It is anticipated that additional aircraft data from NOAA (P-3 Orions and G-IV jet) and NASA (Global Hawks) will be collected during the 2013 Atlantic hurricane season and will enhance the robustness of the observational component of this dissertation. Since the timing of diurnal pulses is quite predictable in both time and space, aircraft missions can be designed with specific takeoff times and flight tracks to optimize sampling of these features. Specific effort will be made to sample TC diurnal pulses during various stages of their evolution [i.e. at both smaller radii (<200 km) near the time of sunset and larger radii (300-500 km) several hours after sunset, as well as at various levels of the atmosphere. The P-3 Orions (flying at ~5,000-12,000 ft) will provide flight-level data, GPS dropwindsonde data, and tail Doppler radar data from ~500m to 14 km. The NOAA G-IV will provide flight-level data, dropwindsonde data from 41,000-45,000 ft to the surface, and tail Doppler radar data from ~500m to 14 km. Finally, the NASA Global Hawks can provide critical information regarding diurnal variations in temperature at the top of the cirrus canopy from a combination of flight level and dropwindsonde

data. Three-dimensional wind information will also be obtained from the TWiLiTE wind lidar flying aboard one of the NASA Global Hawks (pending successful aircraft integration).

c. Model Simulations

A model-based examination of the TC diurnal cycle will also be conducted using analyses from a Hurricane Nature Run (HNR) created using the Joint OSSE Nature Run and WRF model (Nolan et al. 2013). The HNR utilized WRF ARW 3.2.1, a fully compressible, Eulerian, and non-hydrostatic research model initialized using global analysis fields from the European Centre for Medium-Range Weather Forecasts (ECMWF) global forecast model. The HNR is on a 27 km grid (with nesting to 9 km, 3km, and 1 km) and includes 60 vertical levels over a region of the tropical North Atlantic. Physics packages include: Kain-Fritch cumulus parameterization on the 27 km and 9 km grids, 6-class, double-moment microphysics (WDM6), the new RRTM advanced longwave and shortwave radiation schemes (with radiation called every 6-min), the Yonsei University (YSU) planetary boundary layer (PBL) scheme with TC-relevant modifications to the enthalpy coefficient (Ck) and drag coefficient (Cd), and a simple mixed layer scheme for representing ocean cooling under the simulated storm. The output from the WRF/ECMWF nature run includes all WRF state variables, diagnosed surface fields, and all physics tendencies (i.e. boundary layer/friction, cumulus, and radiation), 3-D fields saved every 30-min on the 27 km, 9 km, and 3 km grids, and 3-D fields saved every 6-min on the 1 km grid.

Subsequent to the HNR evaluation, output from a WRF TC simulation (TC TBD) and the Three-Dimensional Vortex Perturbation Analysis and Simulation (3DVPAS) will be analyzed. 3DVPAS is a collection of programs and subroutines, written entirely in Matlab, which can be used to analyze the behavior and evolution of axisymmetric vortices with arbitrary velocity and temperature profiles (Nolan and Montgomery 2002, Nolan and Grasso 2003, Nolan and

Montgomery 2002, and Nolan 2004, Hodyss and Nolan 2006). The objective of these efforts will be to investigate the reproducibility of the TC diurnal findings that result from the HNR and WRF TC analyses and carry out sensitivity experiments to elucidate the mechanisms that drive the TC diurnal cycle (see Sec. 4)

3. Preliminary Results

a. Development of the Tropical Cyclone Diurnal Cycle Tracking Algorithm

The original motivation for the development of the TC diurnal cycle 6-hr IR BT satellite imagery was to simply document spatial changes in the TC cloud field over time. Prototype versions of this technique were used to examine Hurricane Katrina on 28 August 2005, several hours prior to its landfall in Louisiana. A clear cooling trend in the IR cloud tops (~10-60^{o}C) was apparent in the periphery of the storm from 1145-1745 UTC that day and exhibited a remarkable circular shape. However, it was not evident at the time that this circular feature was an evolving and perhaps fundamental component of mature TCs. Additional TC cases were recently examined and revealed similar patterns in the cloud field. This effort led to refinements in the TC diurnal cycle satellite algorithm and enhancement table described in Sec. 2a that include the use of the 10.7 μm IR window channel on geostationary satellite platforms (e.g. GOES) and 6-hr image differencing to track the diurnal pulse signal. The TC diurnal cycle IR satellite imagery developed as part of this dissertation provides much of the motivation for the investigation of the various aspects of TC diurnal cycle.

b. Tropical Cyclone Diurnal Cycle Case Study (2007 Hurricane Felix)

Figure 4 shows an example of the TC diurnal cycle for 2007 Hurricane Felix on 03 September while it was weakening from a major category 5 to category 4 hurricane. The GOES

IR imagery suggests a rapidly expanding cirrus canopy in all quadrants from 1215-1815 UTC and asymmetries were clearly evident in the IR cloud field from R=100-300 km during this time. These asymmetries were mainly associated with a large area of cold cloud tops (-50 to -70^{o}C) in the western and northern semicircles of the storm that appeared to be separating from the inner core region during the morning hours (Fig. 4, upper left; R=~150 km). By the early afternoon local time (Fig. 4, upper right), this arc of cold cloud tops had propagated to a radius of ~250-350 km and an expanding gap of relatively warmer cloud tops (~-30 to -40^{o}C) was evident between this feature and the storm's inner core.

Figure 4 also shows GOES IR differencing imagery that depicts 6-hr changes in the storm's IR temperature field from 0615-1215 UTC. The imagery indicates a circular ring (i.e. diurnal pulse; yellow to pink shading) in the cloud field at approximately R=150-250 km that had cooled as much as 20-50^{o}C during this 6-hr period, with areas of warming (cyan to blue shading, 5-30^{o}C) evident behind the diurnal pulse in the inner ~150 km. By 1815 UTC that day (Fig. 4, lower right panel), the diurnal pulse had propagated to a radius of ~250-350 km from the center and a broad circular area of warming inner core cloud tops (5-40^{o}C) was located on its inner edge at R=~50-200 km. Interestingly, the arc-like feature of radially propagating cold cloud tops previously noted in the GOES IR satellite imagery was also coincident with the position of the diurnal pulse in the differencing images. This suggests that it was, in fact, linked to the diurnal pulse seen propagating away from the storm that day. Although the diurnal pulse evolution is somewhat evident in the GOES IR images (Fig. 4, upper panels), details and subtleties of its structure and position are better elucidated in the GOES IR differencing images (Fig. 4, lower panels).

The 37 and 89/91 GHz microwave satellite images (from the NASA Aqua and DMSP satellites) shown in Fig. 5 are within ~1.5-h of the image times shown in Fig. 4 and confirm that the arc of cold cloud tops (i.e. diurnal pulse) in the western and northern semicircles of Felix was associated with outwardly expanding deep convection and was not just a shallow layer of cirrus outflow. This feature was denoted by cyan to pink shading (37 GHz) and brightness temperatures ranging from 175-250 K (89 and 91 GHz) in the microwave imagery and was positioned ~175-225 km from the storm center at 1348 UTC (Fig. 5, left panels). By 1829 UTC, it was located at radii ranging from ~210-290 km (Fig. 5, right panels). Additional microwave satellite overpasses from NASA TRMM and other DMSP satellites confirmed this radial expansion (not shown). This is a significant observation and suggests that the TC diurnal cycle may be manifested in a deep layer of the TC environment and therefore may be an important influence on TC structure and possibly even intensity.

The outwardly propagating diurnal pulse and marked warming of the cloud tops at radii inside of the pulse appear to be key elements of the TC diurnal cycle and suggest that it has a radially dispersive nature. The structure of this propagating feature also suggests that minima and maxima associated with the TC diurnal cycle (e.g. cirrus canopy areal coverage, convection and precipitation) cannot be adequately described in terms of time alone. Instead, the TC diurnal cycle is better described in terms of both time and space. In order to effectively capture this diurnal signal, azimuthal calculations of GOES IR brightness temperatures and 6-hour IR brightness temperature differences were generated for Hurricane Felix every 3-hr from 01 Sep 2045 LST to 04 Sep 0145 LST at 100-600 km radii from the storm center. It should be noted that the 200-850 hPa vertical shear was quite low (0.5-6 m s^{-1}) throughout this period and consistently below the maximum shear criteria (7.5 m s^{-1}) discussed in Sec. 2.

Figure 6 (top panel) shows a time series of azimuthal mean IR brightness temperature (300, 400, and 500 km radii) for Felix from 01-04 September, while the lower panel shows the identical time period, only for calculations of 6-hr IR brightness temperature differences. The former azimuthal calculations focus on the magnitude of IR brightness temperature fluctuations at various radii, while the latter calculations focus on the amplitude of this signal. There is some indication that the amplitude variability provides a more robust depiction of the TC diurnal cycle and is discussed further in Sec. 3c. A clear maximum cooling in the R=300-500 km satellite IR field is evident in both plots from ~1100-2100 LST, followed by a distinct maximum in warming from ~2300-0700 LST. The oscillatory nature of this cooling and warming is quite regular from day to day in these plots and suggests the repeatability of this phenomenon. Also of note is the apparent phase shift in the timing of the diurnal cycle at the various radii (i.e. the peak cooling/warming tended to progress radially outward in time from 300-500 km). These trends suggest that the TC diurnal cycle signal began at the innermost radii (e.g. 150-200 km, not shown) and propagated to peripheral radii at a speed of ~5-10 m s^{-1} during the course of several hours.

c. Tropical Cyclone Diurnal Cycle Database Analyses

A spectral analysis of the entire 10-yr dataset of both IR brightness temperature and 6-hr brightness temperature difference satellite imagery was then performed to identify signals of the TC diurnal cycle at various radii from the storm center and confirm the cyclic nature of this phenomenon as suggested by the 2007 Hurricane Felix case. Figure 7 shows a spectral analysis of the 6-hr brightness temperature difference imagery from R=100-600 km and corroborates some of the findings from Kossin (2002). A clear diurnal cycle (1 cycle per day) is evident in the IR brightness temperature field that appears to be more robust at peripheral radii (e.g. 200+

km), yet is not as readily detectable at 100 km. Unlike the findings in Kossin (2002), no prominent semi-diurnal (2.0 cycles per day) signal was found at R=100 km in the current dataset. This suggests that if a semi-diurnal cycle is indeed present in TCs at this inner radius, it may either not occur in major hurricanes or is just not readily detectable in the environments of these stronger storms. Interestingly, Fig. 7 shows that even at the 200 km radius, the TC diurnal cycle signal is prominent, though it appears to be strongest at the 300 and 400 km radii. The diurnal cycle power spectrum also indicates that this phenomenon is a prominent feature even at large radii (e.g. 500-600 km), far removed from the convective TC inner core region. It should be noted that the spectral analysis of the IR brightness temperature fields (not shown) produced a coherent, yet slightly less robust diurnal signal. This suggests that the IR brightness temperature differencing technique may be relatively less sensitive to short-term trends in TC intensity and is therefore better able capture the TC diurnal cycle signal.

Based upon the diurnal signal indicated in the spectral analysis of the 2001-2010 dataset, azimuthal mean 6-hr IR brightness temperature differences were calculated at the 400 km radius for a subset (12 storms) of the 31 North Atlantic major hurricanes examined in this study (Fig. 8). These select cases are representative of the larger storm sample and were chosen to illustrate the cyclic nature of the TC diurnal cycle. Each time series represents a continuous 72-hr snapshot for each storm and was examined relative to both LST and hours after sunset in order to optimally capture this diurnal signal. Figure 8 shows that a well-defined TC diurnal cycle with very clear and predictable oscillations in the satellite IR brightness temperature fields emerges, even when numerous TCs are examined. Given the robustness of the TC diurnal signal depicted in Figs. 7 and 8, mean statistics will be calculated from 31 major Atlantic hurricanes from 2001-2010 using the selection criteria described in Sec. 2.

d. Tropical Cyclone Diurnal Cycle NOAA G-IV Aircraft Data

The NOAA Hurricane Research Division conducted two Diurnal Cycle Experiment missions into 2011 Hurricane Katia with NOAA's G-IV high altitude jet. Figure 9 shows the star pattern that was flown on 06 September and indicates fairly extensive GPS dropwindsonde coverage in the environment of the storm and in the region of the diurnal pulse. Both the dropwindsonde and G-IV tail Doppler radar data collected on 06 and 07 September will be used to examine the 3-dimensional environment outside, within and inside the radius of the diurnal pulse that is indicated in the GOES 6-hr IR brightness temperature differencing imagery. Preliminary results show unusual temperature and humidity profiles, as well as outflow patterns in the vicinity of the diurnal pulse and will be investigated in detail. It is anticipated that additional aircraft data from NOAA (P-3 Orions and G-IV jet) and NASA (Global Hawks) will be collected during the 2013 Atlantic hurricane season and incorporated into this dissertation.

e. Tropical Cyclone Diurnal Cycle Modeling

Preliminary analyses of a *HNR* (Nolan et al. 2013) suggest that aspects of the TC diurnal cycle are evident in the simulated model fields. Figure 10 depicts radius-height cross-sections and shows a 24-hr time series (at 3-hourly increments) of azimuthally averaged (top panels) log of q condensate and (bottom panels) radiation tendency and include contours of vertical velocity. Net cloud top cooling is evident from 0000-0900 UTC in the simulation and appears to be coincident with the development of a marked increase in q condensate and vertical velocity at R=~150 km. By 0600 UTC, this trend of enhanced q condensate and vertical motion outside of the inner core region is clearly evident at R=~150-175 km and appears to propagate radially outward over the next several hours. By 2100 UTC, this region of apparently enhanced convection has progressed to R=~250-275 km and is remarkably similar to the outward

propagating diurnal pulses that have been noted in the GOES IR satellite imagery. The possible connection between diurnally-driven changes in radiation at the level of the TC canopy and outward propagating signals of enhanced q condensate and vertical motions will be investigated in detail. Additional model parameters such as radial outflow and canopy-level condensates will also be examined in the context of these other parameters. Results from this effort will be examined in the context of a WRF TC simulation carried out at U Albany (TC TBD) to ascertain the repeatability of the findings in a model framework that is representative of operational mesoscale TC forecast models. The 3DVPAS model will include a synthetic hurricane vortex and a prescribed diurnal-like heating cycle (i.e. constant environmental cooling rates with added diurnal solar heating) and will be used to conduct sensitivity experiments that will examine various possible driving mechanisms of the TC diurnal cycle. Results from the HNR will be used guide the prescribed diurnal-like heating cycle that will be tested and evaluated.

4. Discussion

The observational evidence from geostationary and microwave satellites shown in previous sections suggests that the TC diurnal cycle manifests itself as a pulse in the cloud field each day that involves a deep layer of the storm extending from the cirrus canopy down to sub-freezing levels. Although this indicates that the TC diurnal cycle may have an important influence on TC structure and possibly intensity, the exact mechanism(s) forcing this phenomenon is (are) not clear. Several hypotheses have been previously presented that attempt to address the causes for observed fluctuations in atmospheric deep convection. It is hypothesized that one (or possible a combination) of these hypotheses may be driving the observed TC diurnal cycle that is observed. A more detailed analysis of each of the proposed hypotheses is required to assess their merit.

a. Convectively-driven atmospheric gravity waves

The remarkable symmetry of many of the TC diurnal pulses that were observed in this study invoked the image of a "rock thrown into a pond" and hence some kind of propagating gravity wave feature. The following hypothesis is presented regarding the possible link between convectively generated gravity waves and observed TC diurnal pulses: during the day, gravity waves are generated in the TC inner core and propagate upward into the stratosphere. During this time, convectively generated gravity waves (e.g. Pfister et al. 1993) would generally remain undetectable by conventional observations (e.g. satellite imagery). However, it is possible that rapid cooling at the level of the TC cirrus canopy near the time of sunset could generate a temperature profile (i.e. inversion) that would be capable of reflecting these convectively generated gravity waves (Tripoli and Cotton 1989). During this time, these trapped gravity waves would likely intensify in the troposphere as they propagate away from the storm close to the level of the cirrus canopy and would become more readily detectable (e.g. via satellite imagery) as they move through this cloud layer. The propagation speed of TC diurnal pulses that have been observed, however, is quite slow (~5-10 m s^{-1}) compared to previously described gravity waves forced by cumulonimbus convection and associated with deep tropospheric circulations (e.g. ~30 m s^{-1}, Tripoli and Cotton 1989). This is different from the Tripoli and Cotton (1989) scenario, which described the initiation of widespread convection by the horizontal dispersal of vertical motion due to trapping. This hypothesis suggests the creation of a convectively coupled gravity wave, which may then move slower than a deep gravity wave, but nevertheless resonates with tropopause-level reflections. This idea would be consistent with those of Lindzen and Tung (1976) who suggested that wave CISK can be viewed as wave over-reflection off of an unstable layer. This may suggest that CISK-like convective coupling to

gravity waves might be enhanced by the radiative destabilization at sunset. These ideas will need to be studied both observationally and theoretically and will include an examination of spatial and temporal trends of vertical motions and water vapor condensate in the storm environment.

b. Radiatively reduced outflow resistance

Recent experiments by Tripoli (personal communication) have indicated that the outflow resistance measured by a modified form of Inertial Available Kinetic Energy (IAKE) is tied intrinsically to the potential vorticity of the outflow layer. When the potential vorticity differences between the TC inner core region and surrounding environment are small, IAKE tends toward zero or becomes positive (Mecikalski and Tripoli 1998). The potential vorticity of the outflow layer, in turn, is tied to the static stability of that layer, which is modulated diurnally, particularly when filled with outflow cirrus. Convective bands, as well as the developing storm convective core are suppressed by outflow resistance (i.e. inertial stability), particularly in the early stages of a TC when the outflow layer has not been strongly modified by the storm's own outflow and so remains particularly resistant to the formation of new outflow. Longwave cooling, beginning just before sunset would act to reduce $\frac{d\theta}{dz}$ at the level of the outflow layer (possibly to near-zero values), thus reducing the potential vorticity of the layer and so increasing the modified IAKE, perhaps making it actually positive. This would lead to the release of outflow, and a response to the convection below, previously limited by the outflow resistance. Tripoli has numerically simulated and quantified this outflow response to be significant in the storm genesis stage. Observations and model analyses of the potential temperature and potential vorticity evolution in the outflow layer should be made to supply confirmation of this effect.

c. Cloud-cloud-free differential heating mechanism

Gray and Jacobsen (1977) described the notion that the cirrus canopy radiationally cools more at night and less during the day than surrounding cloud-free regions. The resulting pressure surfaces created by these temperature contrasts promote enhanced upper-level divergence and low-level convergence during the nighttime and early morning hours and could conceivably promote a period of enhanced upper-level outflow that could force the outward propagating TC diurnal pulses that have been observed moving away from the storm at night. This process would suggest the TC diurnal pulses are, in fact, advectively-driven features and given a fairly symmetric CDO, this outflow "release" could conceivably take on a ring-like appearance as it moves away from the TC inner core. Although Liu and Moncrieff (1998) concluded that this type of process was a secondary influence controlling the convective diurnal cycle in their model simulations, the cloud clusters that they examined were either fast moving or developed randomly in their model domain. It is conceivable that cloud-cloud-free differential heating processes could be more important in a more organized, longer lasting convective system such as a TC. Measurements and model analyses of CDO-level diurnal radiation tendencies and outflow patterns will be conducted to investigate this hypothesis.

d. Direct radiation-convection interactions

This hypothesis was discussed by Kraus (1963), Chen and Cotton (1988), and later by Randall et al. (1991) and offers the idea that during the day, solar warming of the convective region cirrus canopy reduces the local lapse rate and promotes increased static stability in the middle to upper troposphere. Conversely, at night, preferential cooling at the level of the cirrus canopy relative to the lower troposphere decreases the static stability. These diurnal radiative trends would act to enhance convection during the nighttime and early morning hours and could also enhance upper-

level divergence during these times. It is plausible that in the TC peripheral environment (e.g. R=150-200 km), relatively shallow convective areas (e.g. spiral bands) could especially benefit from the reduced mid- to upper-level static stability that direct radiation-convection interaction processes would promote. It is also possible that nighttime and early morning periods of enhanced upper-level divergence could promote the observed TC diurnal pulses by promoting outward radial advection and given a fairly symmetric inner core, could conceivably take on a ring-like appearance as this outflow "release" moves away from the TC inner core. Measurements and model analyses of lower and upper-level tropospheric radiation tendencies and upper-level outflow patterns in the storm environment will be conducted to investigate this hypothesis.

e. Seeder-feeder mechanism

Houze et al. (1981) hypothesized that the enhancement of precipitation in warm-frontal rainbands can result when ice particles from aloft fall into the layer below the -4^{o}C level and aggregate just above the melting level. These "seeder" ice crystals can subsequently, as they descend, help convert cloud water to precipitation via Bergeron-Findeisen processes (Bergeron 1935). Houze et al. 1981 also described a second mechanism by which enhanced mesoscale lifting can increase the amount of "feeder" cloud water by condensation of vapor at low levels. It is possible that ice crystals associated with a radially expanding cirrus canopy in a TC environment (initiated by one of the three processes described in Secs. 4a-d) could help stimulate convection in peripheral rainbands via the former mechanism (i.e. seeder-feeder mechanism). Additionally, mesoscale lift associated with a radially propagating gravity wave of sufficient depth could promote the latter mechanism. Measurements and model analyses of deep

tropospheric water vapor condensate, as well as upper-level ice cloud and outflow patterns in the storm environment will be conducted to investigate this hypothesis.

Although the exact nature of the TC diurnal cycle and associated diurnal pulse are uncertain, more than one of the above hypothesized mechanisms could be acting together in the TC environment to produce this diurnal phenomenon. High resolution numerical modeling analyses could be used to examine each of the proposed TC diurnal cycle driving mechanisms in isolation, as well as the possibility that multiple mechanisms are acting in concert to generate this atmospheric phenomenon.

4. Thesis Plan

1. Introduction
- *1.1 Convective Diurnal Cycle Review*
- *1.2 TC Cirrus Canopy Literature Review*
- *1.3 Gravity Wave Literature Review*

2. Datasets

3. Geostationary IR Image Differencing
- *3.1 Motivation*
- *3.2 Algorithm Description*
- *3.3 Assessment of Alternative IR Differencing Algorithms*

4. TC Diurnal Cycle Case Studies
- *4.1 2005 Hurricane Emily*
- *4.2 2007 Hurricane Felix*
- *4.3 Western North Pacific TC (TBD)*
- *4.4 2013 (anticipated)*

5. TC Diurnal Cycle Diurnal Pulse Satellite Analyses (2001-2010)
- *5.1 Spectral Analysis*
- *5.2 Multi-Storm Composite (3-day cycle)*
- *5.3 UW-CIMSS Tropical Cyclone Upper-Level Divergence*
- *5.4 UW-CIMSS Satellite-Based Objective Dvorak TC Intensity Estimates*

6. TC Diurnal Cycle Aircraft Observations
- *6.1 2011 Hurricane Katia (G-IV)*
- *6.2 2013 Hurricane XX (G-IV and P-3 Orions)*

7. TC Diurnal Cycle Model Analyses

7.1 Hurricane Nature Run and WRF TC Simulation (TC TBD) Description

i. Radiation Analyses
ii. Thermodynamic Analyses
iii. Kinematic Analyses
iv. Convective Analyses
v. TC Metrics Analyses (e.g. MSLP and 1-min max sustained surface wind)
vi. Comparisons with Satellite Analyses (Temporal and Spatial)

7.2 Three-Dimensional Vortex Perturbation Analysis and Simulation (3DVPAS) Sensitivity Testing

i. Sensitivity Testing of a prescribed diurnal cycle simulation (radiation)
ii. 3-D analyses of resulting thermodynamic and wind fields

8. Discussion

8.1 TC Diurnal Cycle Structure
8.2 TC Diurnal Cycle Evolution
8.3 Hypothesized TC Diurnal Cycle Driving Mechanisms

i. Convectively-driven Atmospheric Gravity Waves
ii. Radiatively Reduced Outflow Resistance
iii. Cloud-Cloud-Free Differential Heating Mechanism
iv. Direct Radiation-Convection Interactions
v. Seeder-Feeder Mechanism

8.4 Implications for TCs and Tropical Convection in General

9. Future Work

10. References

5. Future Work Plan

The following describes future work objectives to be included in the final version of this dissertation.

a. Chapter 3

The geostationary infrared brightness temperature differencing imagery will be developed and refined to optimize the detection of the TC diurnal cycle for storms in various ocean basins around the globe. This effort will include: testing 3-hr versus 6-hr IR image differencing, testing 11 μm IR versus 6.7 μm water vapor IR channel differencing and testing

different image enhancements for different geostationary satellite platforms (e.g. GOES, MSG, and MTSAT).

b. Chapter 4

Major hurricane case studies will be expanded beyond 2005 Hurricane Emily to include at least one additional historical North Atlantic TC, at least one historical western North Pacific TC, and potential cases from the upcoming 2013 Atlantic hurricane season. These case studies will examine continuous 72-hr segments of the storm lifecycle in the context of environmental vertical wind shear, distance to land, storm intensity and will include the generation of 3-hourly analyses of storm centered IR brightness and brightness temperature differences that are azimuthally averaged at 100 km increments from R=100-600 km from the storm center.

c. Chapter 5

This section will include multi-storm composites to determine the mean diurnal variations in IR brightness and brightness temperature differences (azimuthally averaged at 100 km increments (R=100-600 km) from the storm center for the 2001-2010 Atlantic major hurricane dataset that is being constructed. The variability of these parameters will be put into a framework of both LST and hours after sunset to determine the mean characteristics of TC diurnal pulses. Additional efforts will include extracting 3-hourly UW-CIMSS upper-level divergence values (at azimuthally averaged radial ranges TBD) and Advanced Dvorak intensity estimates for TCs in the 10-yr dataset for comparison against the satellite brightness temperature data that is being analyzed. Finally, a real-time web page will be constructed to track diurnal pulses in the TC environment in a storm-centered framework and will include IR imagery, IR brightness temperature differencing imagery, and plots of azimuthally averaged brightness temperatures at radii of interest (e.g. 200-500 km) versus time for TCs around the world.

d. Chapter 6

Aircraft missions will be designed and implemented during the 2013 Atlantic hurricane season to gather additional observations in TCs exhibiting diurnal pulsing. These observations will include: GPS dropwindsonde and tail Doppler radar data from NOAA's P-3 Orions and G-IV jet, as well as dropwindsonde data and 3-dimensional wind retrievals from the TWiLiTE lidar aboard NASA's Global Hawk(s).

e. Chapter 7

Data from a HNR (Nolan et al. 2013) has been obtained on a 500 Gb external drive and contains the needed data to conduct the model analyses component of this study. Additionally, the code for running the Three-Dimensional Vortex Perturbation Analysis and Simulation (3DVPAS) has been obtained. The WRF TC Simulation (TC TBD) will require "spin-up" time, but unlike the HNR and 3DVPAS efforts, will provide analyses from an actual simulated North Atlantic hurricane. In-depth analyses of the kinematics, thermodynamics, and radiation in the inner core and surrounding environment of the simulated TC environments from these three models will be conducted to address several the science questions presented in Sec. 1 and hypothesized driving mechanisms discussed in Sec. 4.

f. Chapter 8

The satellite, aircraft and model simulation analysis efforts that are conducted will be integrated into an analysis of the various science questions and hypothesized TC diurnal cycle driving mechanisms that are detailed in Sec. 4.

References

Bergeron, T., 1935: On the physics of cloud and precipitation. *Proc. 5th Assembly U.G.G.I. Lisbon*, **Vol. 2**, p. 156.

Browner, S.P., W.L. Woodley, and C.G. Griffith, 1977: Diurnal oscillation of cloudiness associated with tropical storms. *Mon. Wea. Rev*., **105**, 856-864.

Chen, S., and W.R. Cotton, 1988: The sensitivity of a simulated extratropical mesoscale convective system to longwave radiation and ice-phase microphysics. *J. Atm. Sci*., **45**, 3897-3910.

Cotton, W.R, G. Bryan, S.C. Van Den Heever, 2010: Storm and Cloud Dynamics. Academic Press 809 pp.

Gray, W.M., and R.W. Jacobson, 1977: Diurnal variation of deep cumulus convection. *Mon. Wea. Rev*., **105**, 1171-1188.

Hodyss, D., and D.S. Nolan, 2006: Anelastic equations for atmospheric vortices. *J. Atmos. Sci*., **64**, 2947-2959.

Houze, R.A., S.A. Rutledge, T.J. Matejka, and P. V. Hobbs, 1981: The mesoscale and microscale structure and organization of clouds and precipitation in midlatitude cyclones. III: air motions and precipitation growth in a warm-frontal rainband. *J. Atm. Sci*., **38**, 639-649.

Jarvinen, B.R., C.J. Neumann, and M.A. S. Davis, 1984: A tropical cyclone data tape for the North Atlantic basin, 1886-1983: contents, limitations, and uses. *NOAA Tech. Memo., NWS NHC 22*, 21 pp. (Available at http://www.nhc.noaa.gov/pdf/NWS-NHC-1988-22.pdf)

Kossin, J.P, 2002: Daily hurricane variability inferred from GOES infrared imagery. *Mon. Wea. Rev*., **130**, 2260-2270.

Kraus, E.B., 1963: The diurnal precipitation change over the sea. *J. Atm. Sci*., **20**, 546-551.

Lenz, A., K.M. Bedka, W.F. Feltz, and S.A. Ackerman, 2009: Convectively induced transverse band signatures in satellite imagery. *Wea. And Forecasting*, **24**, 1362- 1373.

Lindzen, R.S, and K-K. Tung, 1976: Banded convective activity and ducted gravity waves. *Mon. Wea. Rev*., **104**, 1602-1617.

Liu, C., and M.W. Moncrieff, 1998: A numerical study of the diurnal cycle of tropical oceanic convection. *J. Atm. Sci*., **55**, 2329-2344.

Mapes, B. E., and R.A. Houze Jr., 1993: Cloud clusters and super- clusters over the oceanic warm pool. *Mon. Wea. Rev*., **121**, 1398–1415.

Mecikalski, J.R., and G. J. Tripoli, 1998: Inertial Available Kinetic Energy and the Dynamics of Tropical Plume Formation. *Mon. Wea. Rev*., **126**, 2200-2216.

Nolan, D.S., R. M. Atlas, K.T. Bhatia, and L.R. Bucci, 2013: Development and validation of a hurricane nature run using the Joint OSSE Nature Run and WRF Model. *J. Adv. in Mod. Earth Syst*. (submitted).

Nolan, D.S., 2004: Mechanics and efficiency of symmetric and asymmetric intensification processes. *Proc. 26th Conference on Hurricanes and Tropical Meteorology, Miami Beach, FL,* Amer. Meteor. Soc.

Nolan, D.S., and M.T. Montgomery, 2002: Nonhydrostatic, three-dimensional perturbations to balanced, hurricane-like vortices. Part I: Formulation, linearized evolution, and stability. *J. Atmos. Sci*., **59**, 2989-3020.

Nolan, D.S., and L.D. Grasso, 2003: Nonhydrostatic, three-dimensional perturbations to balanced, hurricane-like vortices. Part II: Symmetric response and nonlinear simulations. *J. Atmos. Sci*., **60**, 2717-2745.

Nolan, D.S., and M.T. Montgomery, 2002: Nonhydrostatic, three-dimensional perturbations to balanced, hurricane-like vortices. Part I: Formulation, linearized evolution, and stability. *J. Atmos. Sci*., **59**, 2989-3020.

Olander, T.L., and C.S. Velden, 2007: The Advanced Dvorak Technique: continued development of an objective scheme to estimate tropical cyclone intensity using geostationary infrared satellite imagery. *Wea. And Forecasting*, **22**, 287-298.

Pfister, L., K.R. Chan, T.P. Bui, S. Bowen, M. Legg, B. Gary, K. Kelly, M. Proffitt, and W Starr, 1993: Gravity waves generated by a tropical cyclone during the STEP tropical field program. *J. Geophys. Res*., **98**, 273-8638.

Tripoli, G. J., and W.R. Cotton, 1989: Numerical study of an observed orogenic mesoscale convective system. Part 1: Simulated genesis and comparison with observations. *Mon. Wea.Rev*., **117**, 273-304.

Weickmann, H.K., A.B. Long, and L.R., Hoxit, 1977: some examples of rapidly growing oceanic cumulonimbus clouds. *Mon. Wea. Rev*., **105**, 469-476.

Velden, C.S., B. Harper, F. Wells, J.L. Beven II, R. Zehr, T. Olander, M. Mayfield, C. Guard, M. Lander, R. Edson, L. Avila, A. Burton, M. Turk, A. Kikuchi, A. Christian, P. Caroff, P. McCrone, 2006: The Dvorak tropical cyclone intensity estimation technique: A satellite-based method that has endured for over 30 years. *Bull. Amer. Meteor. Soc*., **87**, 1195-1210.

Yang, G, and J. Slingo, 2001: The diurnal cycle in the tropics. *Mon. Wea. Rev*., **129**, 784-801.

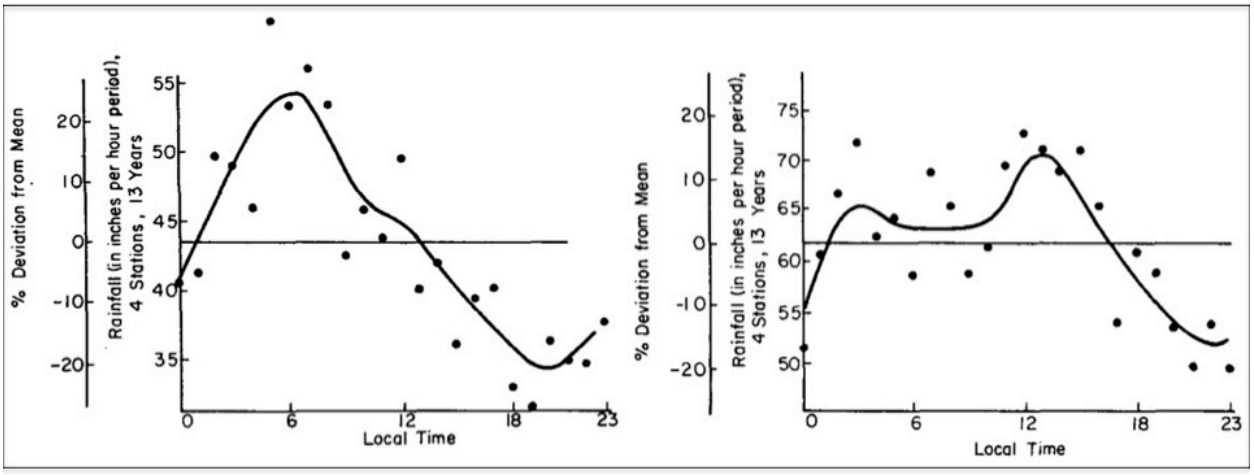

Fig 1: Precipitation curves for (left) small islands (Truk, Wake, Majuro, and Johnston Island) and (right) large islands (Koror, Yap, Guam, and Ponape) during spring (March-May). Data was obtained over the region of the Western North Pacific from 1961-1973 (from Gray and Jacobson 1977).

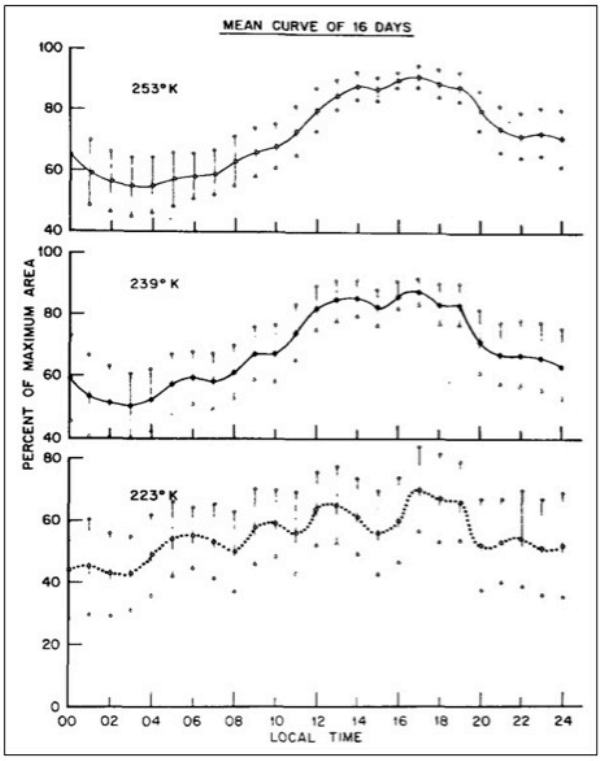

Fig. 2: A composite diurnal oscillation of eight storms on 16 days (1974-1975). Storm areas at each isotherm were normalized to the corresponding threshold maximum area for the day, composited according to local mean solar time and then averaged. Ninety-five percent confidence intervals are shown. Due to the variability of the occurrence of the maximum areas from storm to storm, these curves do not pass through 100% (from Browner et al. 1977).

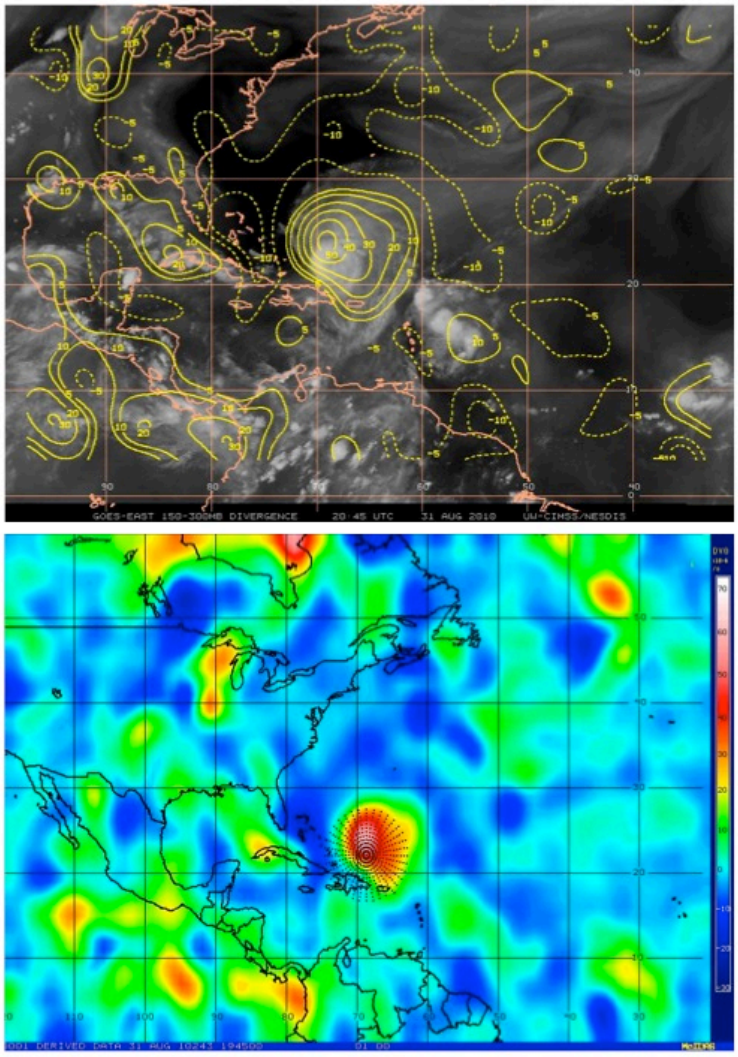

Fig 3: (Top) UW-CIMSS 150-300 hPa upper-level divergence analysis for 31 Aug 2010 2045 UTC. Regions of positive (negative) upper-level divergence are indicated by the solid (dashed) curves. The region of enhanced divergence located northeast of Hispaniola was associated with Hurricane Earl. The bottom panel shows the same upper-level divergence analysis after conversion to a McIDAS AREA file (positive divergence is indicated by the green to pink shading). Divergence values were calculated azimuthally around the storm from R=0-600 km and are indicated by the black circles.

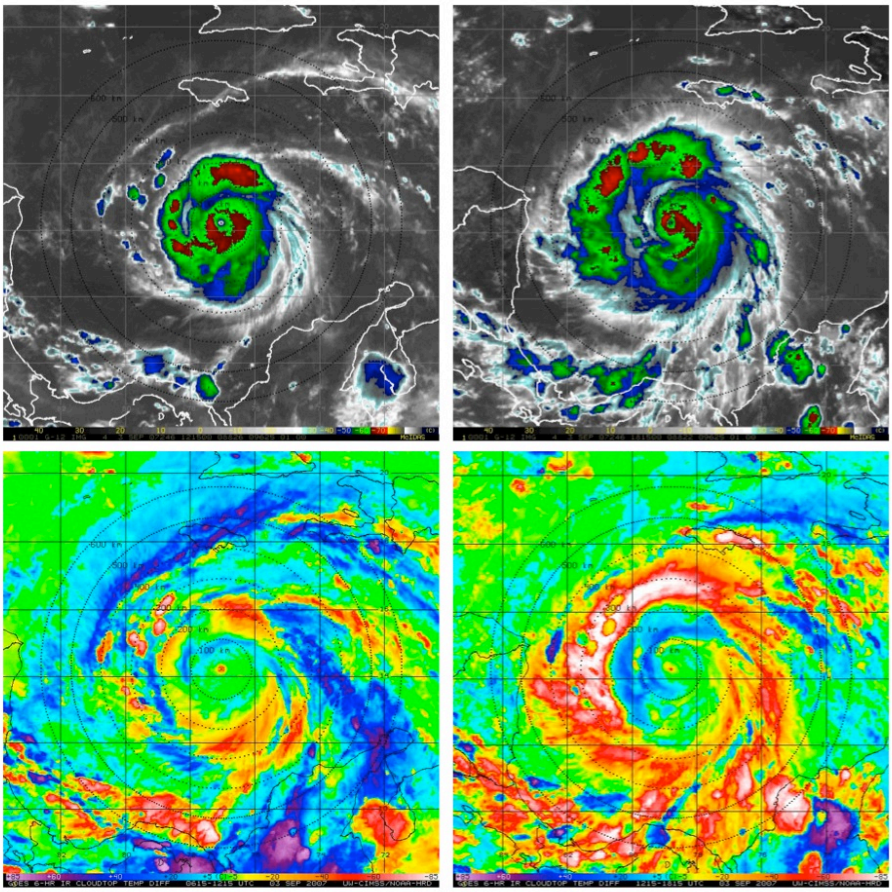

Fig. 4: (Upper panels) GOES IR imagery showing 2007 Hurricane Felix on 03 Sep valid for (left) 1215 UTC and (right) 1815 UTC. The corresponding 6-hr GOES IR brightness temperature differencing images for these times are shown in the lower panels. The yellow to pink shading indicates a diurnal pulse "cool ring" propagating away from the storm during this 6-hr period. 100-600 km range rings (black dashed curves) from the TC center are overlaid on each of the satellite images). Lines of latitude and longitude are marked at 2 degree intervals.

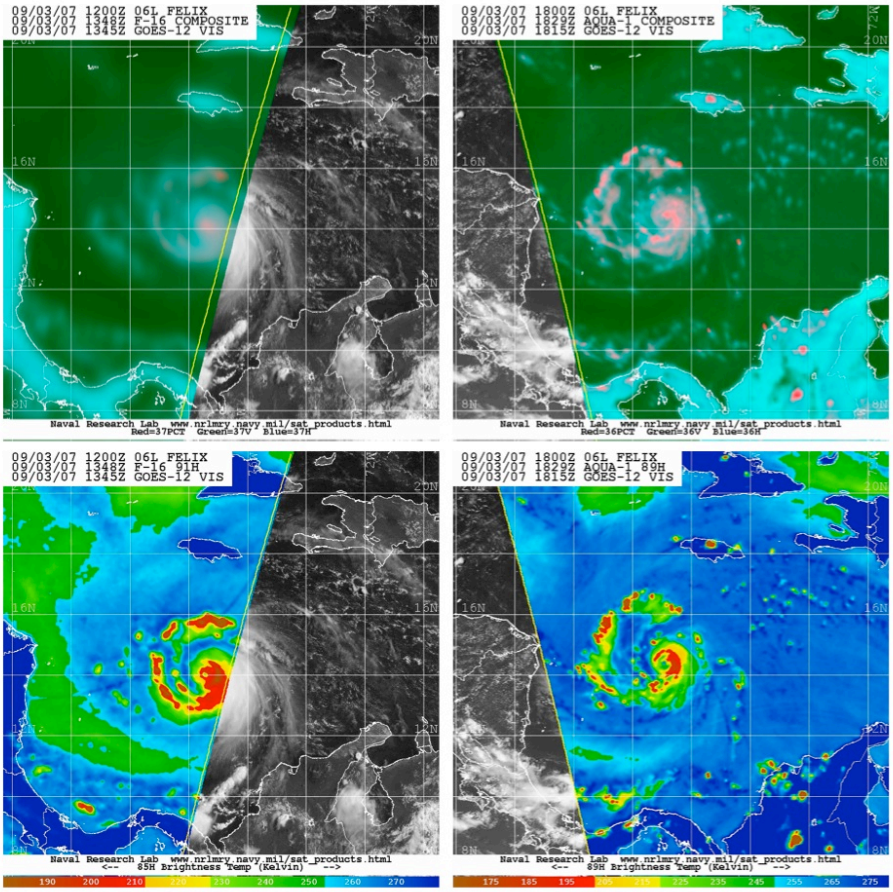

Fig. 5: (Upper panels) DMSP and NASA Aqua 37 GHz composite microwave satellite imagery for 2007 Hurricane Felix on 03 Sep valid for (left) 1348 UTC and (right) 1829 UTC. The corresponding 89/91 GHz microwave images for these times are shown in the lower panels. Note that the microwave overpass times are within 90-min of the respective GOES images shown in Fig. 1 and that areas outside of the satellite swath were supplemented by GOES-12 visible imagery. Lines of latitude and longitude are marked at 2 degree intervals.

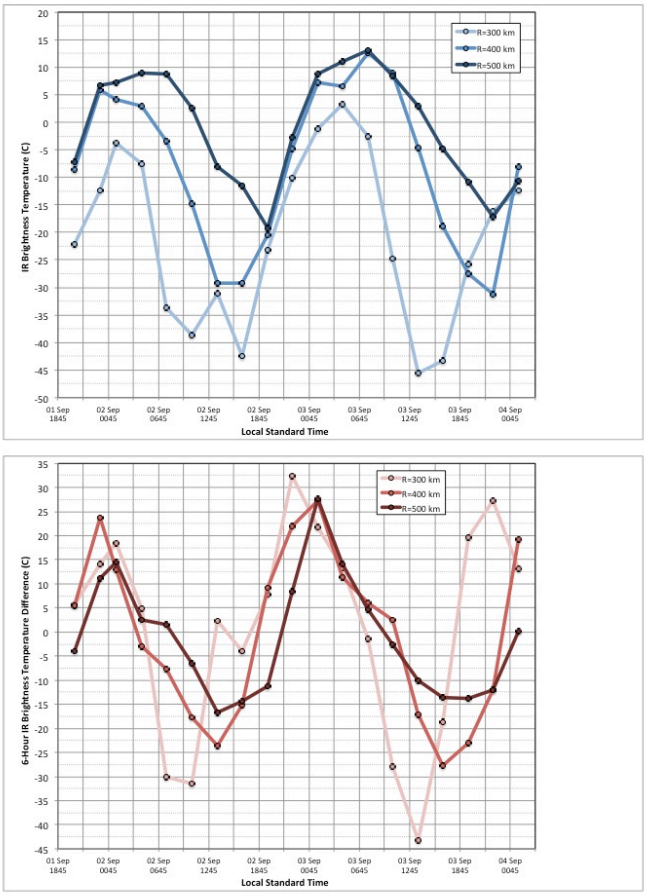

Fig. 6: Azimuthally averaged 3-hourly GOES-12 (upper panel) IR brightness temperatures and (lower panel) 6-hr brightness temperature differences at the 300, 400, and 500 km radii around 2007 Hurricane Felix from 01 Sep 2045 LST – 04 Sep 0145 LST.

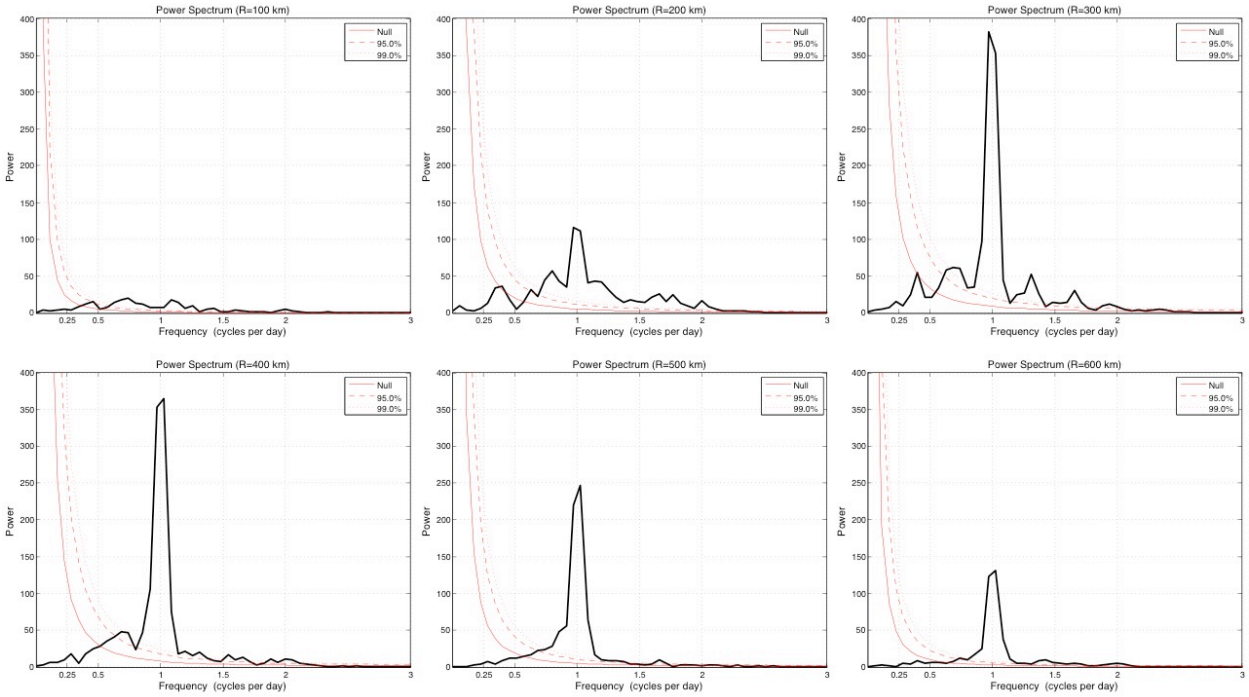

Fig. 7: Power spectrum of azimuthally averaged GOES-12 infrared 6-hr brightness temperature differences for the 2001-2010 North Atlantic major hurricanes that were investigated (R=100-600 km). The red curved lines indicated various confidence levels in the analyses.

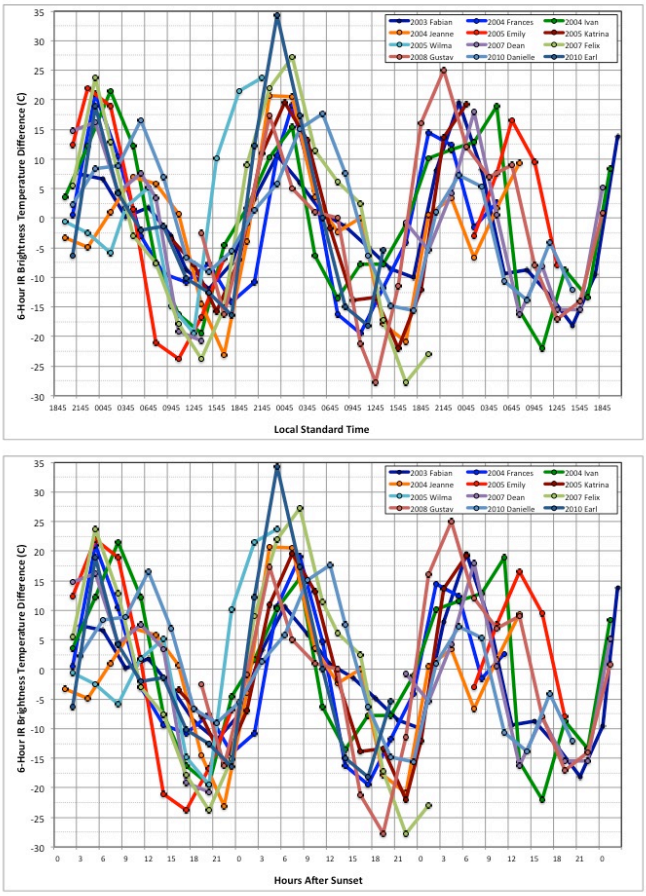

Fig. 8: Azimuthally averaged 3-hourly GOES-12 6-hr brightness temperature differences for several North Atlantic major hurricanes at the 400 km radius relative to (upper panel) local standard time and (lower panel) hours after local sunset.

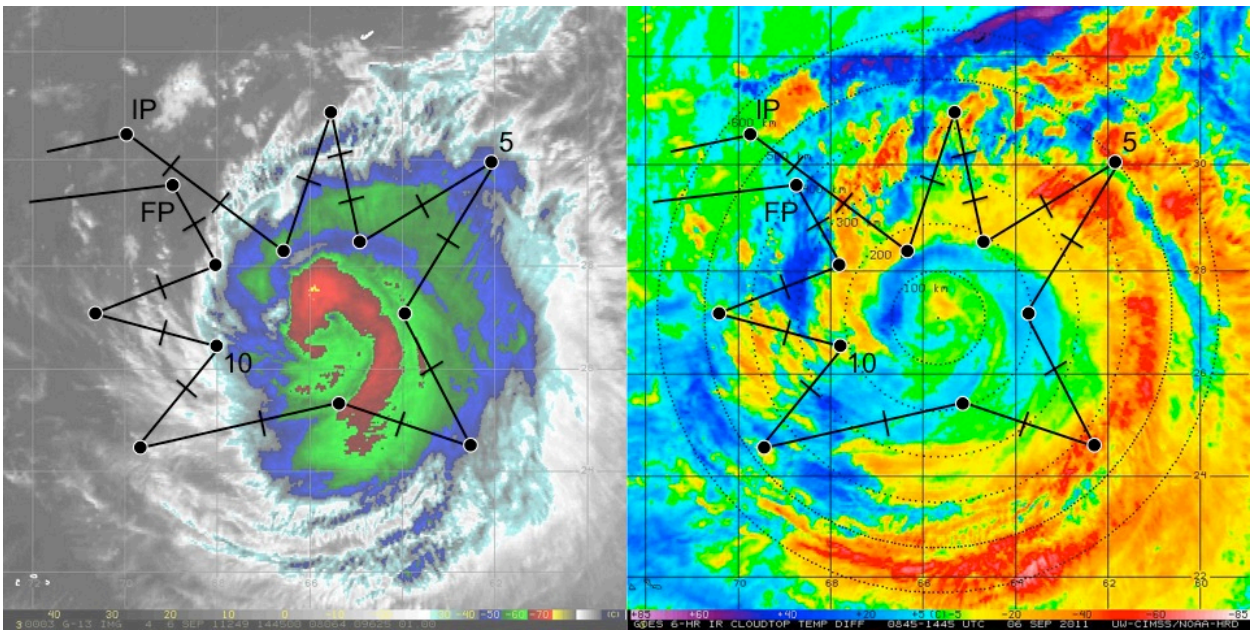

Fig. 9: 2011 (Left) GOES enhanced IR satellite imagery and (right) GOES 6-hr IR brightness temperature differencing (0845-1445 UTC) showing Hurricane Katia on 06 September at 1445 UTC. An evolving TC diurnal pulse is indicated in the right panel and seen as a quasi-symmetric ring of cooling cloud tops in the image (yellow to red shading). Cloud top warming (blue shading) is indicated on the inner edge of the diurnal pulse. The black curves show the NOAA G-IV flight track as it conducted HRD's TC Diurnal Cycle Experiment around the storm. Black circles and hash marks denote GPS dropwindsonde launch points. The initial (IP) and final (FP) points of the mission are also overlaid.

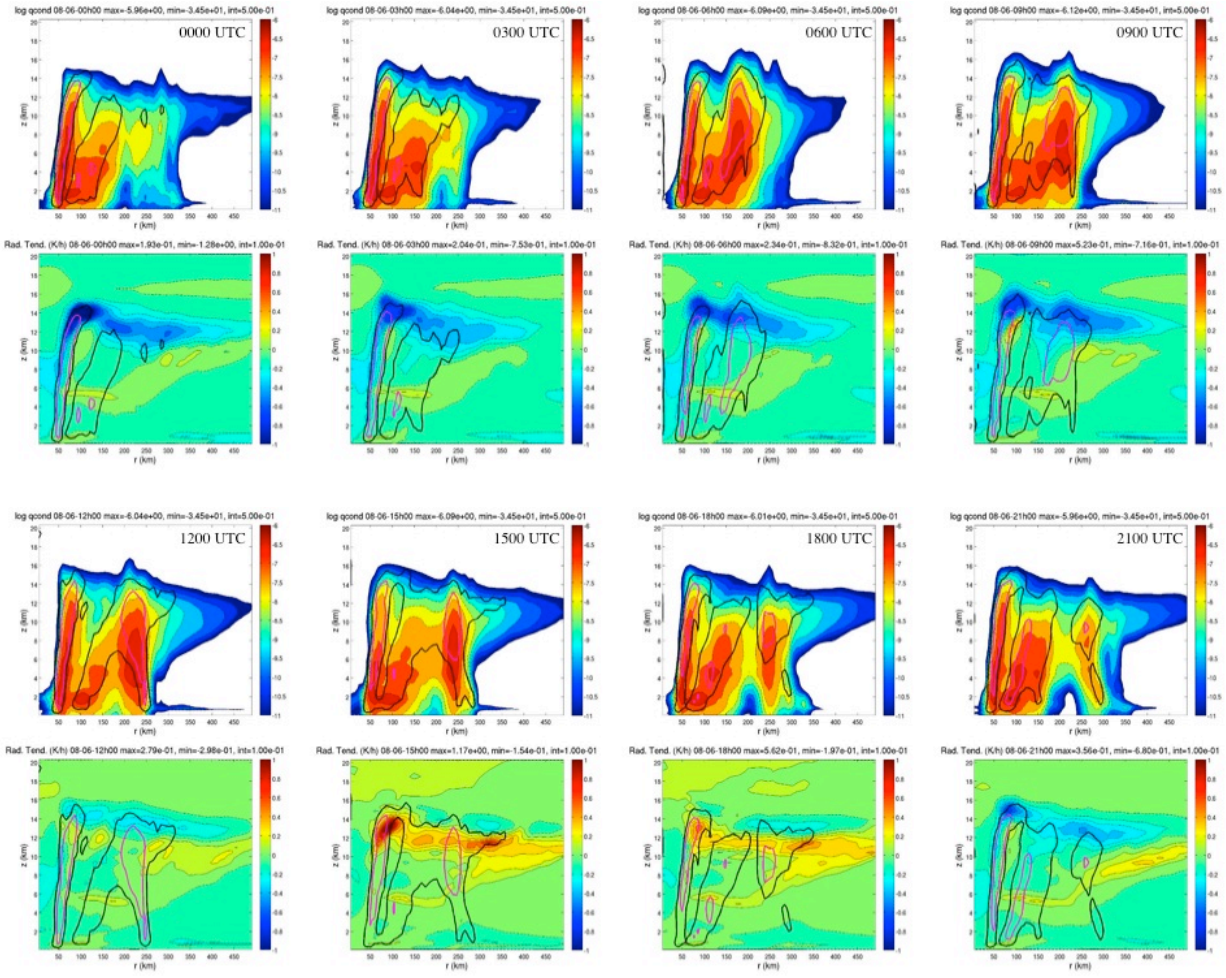

Fig. 10: Radius-height cross-sections showing a 24-hr time series (at 3-hourly increments) of azimuthally averaged (top panels) log of q condensate and (bottom panels) radiation tendency (shortwave plus longwave). The black (magenta) curves show areas of enhanced (maximum) vertical motions for each time period. Model data is from Hurricane Nature Run described in Sec. 2c (Nolan et al. 2012).